NANOSYSTEMS: PHYSICS, CHEMISTRY, MATHEMATICS, 2013, 4 (3), P. 357–362

DIELECTRIC STUDIES OF NANOCRYSTALLINE MANGANESE TUNGSTATE

N. Aloysius Sabu[1], K. P. Priyanka[1], Smitha Thankachan[2], Anu Tresa Sunny[3], E. M. Mohammed[2], O. P. Jaseentha[1], Thomas Varghese[1,*]

[1] Nanoscience Research Centre (NSRC), Department of Physics, Nirmala College, Muvattupuzha - 686 661, Kerala, India

[2] Department of Physics, Maharaja's College, Ernakulam - 682 011, Kerala, India

[3] School of Chemical Sciences, MG University, Kottayam - 686 560, Kerala, India

*nanoncm@gmail.com

PACS 81.16.Be, 81.07.Bc, 73.63.Bd

The dielectric properties of monoclinic manganese tungstate have been studied as a function of frequency and temperature. It was found that the dielectric constant and dielectric loss for all temperatures had high values at low frequencies which decreased rapidly as frequency increased attaining a constant value at higher frequencies. The a.c. conductivity increased as frequency increased, conforming small polaron hopping. As temperature increased, the values of the a.c. conductivity are shifted to higher values. Higher values were also obtained when the particle size decreased. These properties make the nano-sized $MnWO_4$ as a promising material for fabricating humidity sensors.

Keywords: dielectric studies, manganese tungstate, nanoparticles, polaron hopping.

1. Introduction

Nanostructured tungstate materials have aroused much interest because of their luminescent behavior, structural properties and potential applications. Manganese tungstate ($MnWO_4$) is a promising material for fabricating humidity sensors due to its appropriate bulk electrical conductivity. Humidity sensors are important in many areas like meteorology, medicine, food production, agriculture, industrial and general household applications [1–3]. This compound is antiferromagnetic, with a magnetic moment of 5.44 μ_B and a Neel temperature 14.4 K [4]. The various methods employed for the synthesis of $MnWO_4$ include the sol-gel method [2], chemical reaction in a molten salt solution, grinding in a vibrating mill, thermal treatment of a metathesis reaction product [5] and the solvothermal method [6]. In the present work, we report a successful room temperature synthesis of manganese tungstate nanoparticles, adopting careful control of the reaction kinetics of aqueous precipitation.

2. Experimental

Manganese chloride and sodium tungstate (99.9% purity) were purchased from Sigma Aldrich Chemicals and were used without further purification. Nanosized powders of manganese tungstate were prepared by reacting aqueous solutions of manganese chloride and sodium tungstate (0.001 M each) at room temperature keeping the pH = 7. The precipitate formed was centrifuged, filtered and washed with distilled water a number of times, and dried in an oven to obtain manganese tungstate as a fine powder. The precursor

was annealed in air at 450 ° C, 600 ° C and 750 ° C for 3 hours. The structural characteristics of the synthesized manganese tungstate nanoparticles were then studied by X-ray powder diffraction (XRD) using Bruker D8 Advance X-ray diffractometer (λ = 1.5406 Å). The powder was consolidated in the form of cylindrical pellets of diameter 11 mm and thickness d = 1.2 mm at a pressure of $\sim$ 5 GPa using a hydraulic press. Both faces of the pellets were coated with an air-drying silver paste. Dielectric measurements, as a function of frequency ranging from 100 Hz $\sim$ 15 MHz were measured at selected temperatures from 300 K — 425 K using a LCR meter (Wayne Kerr H-6500 model) in conjunction with a portable furnace and temperature controller ($\pm$1 K) using the four probe method. The dielectric constant and a.c. conductivity (σac) were calculated using Eq.(1) and (2) respectively.

$$\varepsilon' = \mathrm{cd}/\varepsilon_0 \mathrm{a}, \tag{1}$$

$$\sigma \mathrm{ac} = \varepsilon' \varepsilon_0 \omega \tan\delta, \tag{2}$$

where a is the face area, c the measured capacitance of the pellet, ε_0 the permittivity of vacuum, ω the angular frequency and tan δ, the loss tangent.

3. Results and discussion

Fig. 1 displays the powder X-ray diffraction pattern of the samples annealed at 450 ° C, 600 ° C and 750 ° C for 3 hours. From XRD patterns, using the Scherrer equation, the size of the particles corresponding to different annealing temperatures were estimated to be 25 nm, 30 nm, and 40 nm for samples M1, M2 and M3 respectively. As the annealing temperature increased, XRD patterns showed much sharper peaks and were due to the larger particle sizes obtained at higher temperatures. The principal 'd' values taken from the JCPDS file No. 80-0135 for $MnWO_4$ are in close agreement with the observed 'd' values.

Fig. 2(A) shows the variation of dielectric constant with frequency for temperatures from 303 K to 423 K of sample M3. It can be seen that the real part of the dielectric constant for all temperatures had high values at low frequencies which decreased rapidly as frequency increased, attaining a constant value at higher frequencies. For 303 K, the value of ε' was 4.07 at 100 Hz, which decreased to 0.057 at 10MHz. At 363 K the values were 22.2 (100 Hz) and 0.16. The corresponding values for 423 K were 57.1 at 100 Hz and 0.186 at 10 MHz respectively. The inset figure 2(A) shows a similar variation for all the samples with different particle sizes, at 303 K, but the values were shifted upward when the grain size decreased. The value of ε' changed from 9057 at 100 Hz to 52.7 at 10 MHz for sample M1 while this quantity changed from 2357.6 (100 Hz) to 17.02 (10 MHz) for sample M2 and from 63.16 (100 Hz) to 0.19 (10 MHz) for sample M3 respectively.

In dielectric nanostructured materials, interfaces with large volume fractions contain a large number of defects, such as dangling bonds, vacancies, vacancy clusters, and microporosities, which can cause a change of positive and negative space charge distribution in interfaces. When subjected to an electric field, these space charges move. When they are trapped by defects, several dipole moments are formed. At low frequencies, these dipole moments are easy to follow by monitoring the variation of the electric field [7–8]. So, the dielectric loss, and hence, the dielectric constant showed large values at low frequencies. As the temperature increased, more and more dipoles were aligned, resulting in an increased dielectric constant for a given frequency [9].

At very high frequencies (MHz), the charge carriers would have moved before the field reversal occurred and thus, ε' decreased at higher frequencies. The nature of the

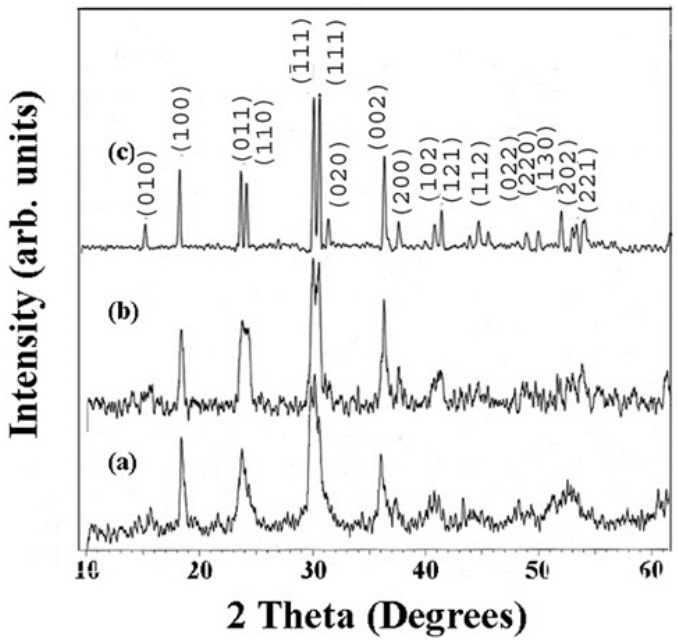

Fig. 1. Shows the XRD pattern of the samples annealed at (a) 450 ° C, (b) 600 ° C and (c) 750 ° C

variation is similar for the other samples, but the values were increased when the grain size decreased. The amorphous nature of the surface, high surface energy, micromechanical stress, surface domain depolarization and domain wall effects were considered as reasons for this variation. Both space charge polarization and reversal of polarization direction contribute significantly to the ε' [10–11]. With increased particle volume, the interfacial volume decreased. Increasing the particle volume also increased the contribution to ε' by electronic relaxation polarization, which occurs mainly inside the particles. Decreasing the interfacial volume diminishes contribution to ε' by space charge polarization and rotation of the direction of polarization, which occur mainly in the interfacial region. As a result ε' decreased as particle size increased.

The variation of tanδ with frequency of sample M3 is shown in Fig. 2(B). The variation of tanδ is similar to that of ε'. For 303 K, tanδ had a value of 4.72 at 100 Hz which decreased to 0.736 at 10 MHz. At 363 K the corresponding change was from 8.63 to 0.73. For 423 K, tanδ had a value of 43.3 at 100 Hz which decreased to 3.38 at 10 MHz. The variation of tanδ with frequency at 303 K for different grain sizes is shown in Fig. 2 (B). At 100 Hz the value was 71.4 for M1 which decreased to 2.20 (10 MHz). For M2 the values were 43.3 (100 Hz) and 3.38 (10 MHz), while for M3, the values were 4.72 (100 Hz) and 0.736 (10 MHz) respectively. In nanophase materials the heterogeneities present in the interface layers produce an absorption current, resulting in dielectric loss. This absorption current decreases with increases in the frequency of the applied field. The hopping probability per unit time increases with increased temperature. Correspondingly the loss tangent also increases with increase of temperatures [12–13]. From X-ray results it was found that the particle size and crystallanity increased as the sintering temperature was elevated. The volume percentage of interface boundaries, defects and imperfections were greatly reduced as the sintering temperature was increased. This explains the increase of tangent loss as the particle size was decreased. The loss in $MnWO_4$ can be explained by the electronic hopping model, which considers the frequency

dependence of the localized charge carriers hopping in a random array of centers. This model is applicable for materials in which the polarization responds sufficiently rapidly to the appearance of an electron on any one site so that the transaction may be said to occur effectively into the final state [14]. At higher frequencies, tanδ becomes almost constant because the electron exchange interaction (hopping) between Mn^{+2} and Mn^{+3} cannot follow the alternatives of the applied a.c. electric field beyond a critical frequency.

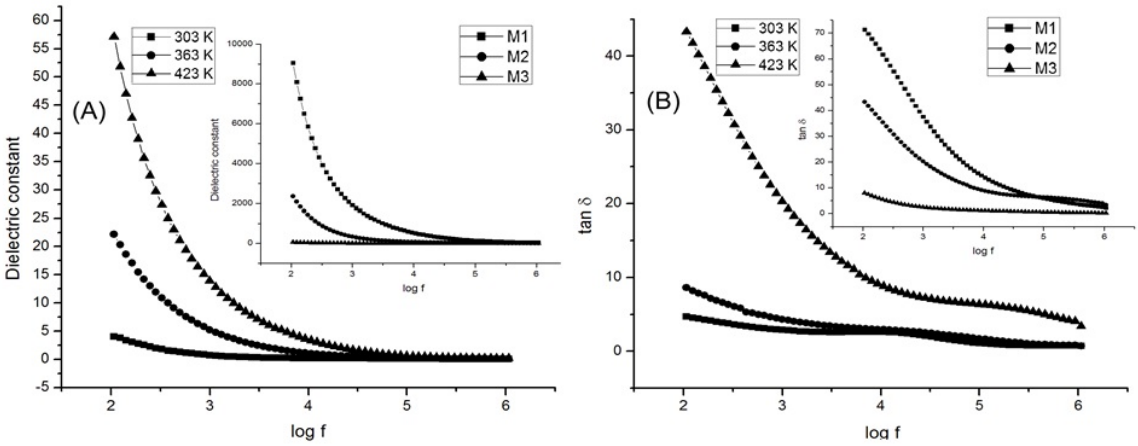

Fig. 2. (A) The variation of dielectric constant with frequency and (B) the variation of tanδ with frequency for temperatures from 303 K to 423 K of sample M3

The variation of the a.c. electrical conductivity as a function of frequency for sample M3 is shown in Fig. 3. At lower frequencies σac had a small value which increased at higher frequencies. The nature was similar for other temperatures but the values were shifted upwards at higher temperatures. For 303 K, σac had a value of 0.0373×10^{-3} S/m at 100Hz which increased to 0.434×10^{-3} S/m at 10 MHz. At 363 K, the corresponding variation was from 0.123×10^{-3} S/m (100 Hz) to 0.71×10^{-3} S/m (10 MHz), while at 423 K, the values were 1.62×10^{-3}S/m at 100 Hz and 3.78×10^{-3} S/m at 10 MHz. The variation of σac with frequency at 303 K for different grain sizes is shown in Fig. 3. At 100 Hz the value was 3.83×10^{-3} S/m for M1, which increased to 6.88×10^{-3} S/m at 10 MHz. For M2, the values were 0.0826×10^{-3} S/m (100 Hz) and 1.15×10^{-3}S/m (10 MHz), while for M3, the figures were 0.0373×10^{-3} S/m (100 Hz) and 0.434×10^{-3} S/m (10 MHz) respectively.

It is clear from the figures that the conductivity increased as the frequency increased, conforming small polaron hopping. Small polaron formation takes place in those materials whose conduction band arise from incomplete 'd' or 'f' orbitals. In $MnWO_4$, both Mn^{+2} and W^{+6} have incomplete 'd' orbitals which are responsible for the formation of small polarons. Also, there is the possibility of conduction due to impurities at low temperatures. The thermoelectric power of $MnWO_4$ has been reported to increases with temperature [4]. At lower temperatures, the a.c. conductivity increases with warming. Dissanayeke et al., observed a similar variation, but at higher temperatures, σac was independant of frequency [15]. In $MnWO_4$, the conduction was due to the exchange interaction (hopping of electrons) between the Mn^{+2} and Mn^{+3}. According to Elliot's barrier hopping model, the ac conductivity is given as Eq.(3),

$$\sigma\mathrm{ac} = \mathrm{n}\pi^2\mathrm{NN}_p\varepsilon'\omega\mathrm{R}_\omega^6/24, \tag{3}$$

where n is the number of polarons involved in hopping, NN_p, proportional to the square of concentration of states, ε' the dielectric constant and R_ω the hopping distance [16]. When the grain size of the sample was reduced the hopping distance increased which increased the conductivity. The conduction in manganese tungstate is due to the hopping and ionic conduction of Mn^+ ions. The high values of σac for particles with small grain sizes are a direct confirmation of the theory.

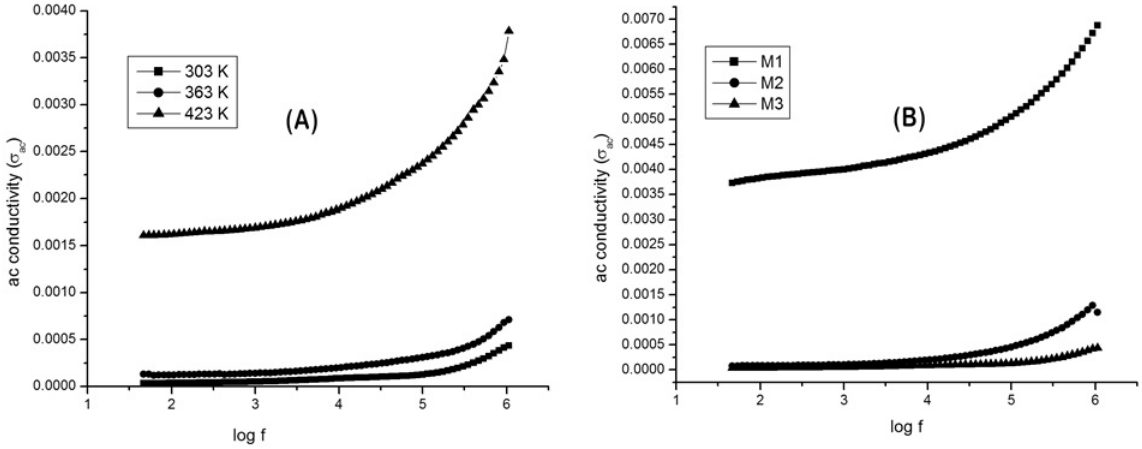

Fig. 3. The variation of a.c. electrical conductivity as a function of frequency

4. Conclusion

$MnWO_4$ nanoparticles with different average sizes were synthesized. The dielectric properties of $MnWO_4$ were determined as a function of frequency from 100 Hz to 10 MHz for temperatures ranging from 303 K to 423 K. At lower frequencies, ε' and tanδ have higher values, while at higher frequencies, the values reach steady lower values. Similar variation was observed when the temperature was raised, but the values were shifted higher. Conductivity increased as frequency increased, conforming to small polaron hopping. The values were shifted upwards when the temperature was raised. The values of ε', tanδ and σac showed considerable increase as the particle size was reduced.

Acknowledgements

The authors are grateful to KSCSTE, Thiruvananthapuram, Kerala and University Grants Commission (UGC), New Delhi for the financial support.

References

[1] E. Traversa, Ceramic sensors for humidity detection: the state of the art and future developments. *Sens. Actuators B*, **23**, P. 135–156 (1995).

[2] W. Qu, W. Wlodarski, J.U. Meyer, Comparative study on micromorphology and humidity sensitive properties of thin-film and thick film humidity sensors based on semiconducting $MnWO_4$. *Sens. Actuators B*, **64**, P. 76–82 (2000).

[3] A.M.E. Suresh Raj, C. Mallika, O.M. Sreedharan, K.S. Nagaraja, MnO-manganese tungstate composite humidity sensors. *Mater. Lett.*, **53**, P. 316–320 (2002).

[4] R. Bharati, R.A. Singh, B.M. Wanklyn, Electrical conduction in Manganese Tungstate. *J. Phys. Chem. Solids*, **43**, P. 641–644 (1982).

[5] M.Jang, T.J.R. Weakley, K.M. Doxsee, Aqueous crystallization of Manganese (II) Group 6 Metal Oxides. *Chem. Mater.*, **13**, P. 519–525 (2001).

[6] S.J. Chen, X.T. Chen, Z. Xue, J.H. Zhou, J. Li, Morphology control of $MnWO_4$ nanocrystals by a solvothermal route. *J. Mater. Chem.*, **13**, P. 1132–1135 (2003).
[7] B. Parvatheeswara Rao, K.H. Rao, Electrical properties of nanocrystalline $AlPO_4$. *J. Mater. Sci.*, **32**, P. 6049–6054 (1997).
[8] C.M. Mo, L. Zhang, G. Wang, Characteristics of dielectric behavior in nanostructured materials Nanostruct. *Mater.*, **6**, P. 823–826 (1995).
[9] T. Kar, R.N. Choudhary, S. Sharma, K.S. Singh, Structural and electrical properties of $Ba_2Na_3RNb_{10}O_{30}$ Ceramics. *Indian J. Phys*, **73A**(4), P. 453–459 (1999).
[10] B. Jiang, J.L. Peng, L.A. Busil,W.L. Zhong, Size effects on ferroelectricity of ultrafine particles of $PbTiO_3$. *J. Appl. Phys.*, **87**(7), P. 3462–3467 (2000).
[11] D.Ravinder, K.Vijayakumar, Dielectric behaviour of erbium substituted Mn–Zn ferrites. *Bull. Mater. Sci.*, **24**(5), P. 505–509 (2001).
[12] S.N. Potty, M.A. Khader, Dielectric Properties of nanophase Ag_2HgI_4 and Ag_2HgI_4-Al_2O_3 nanocomposites. *Bull. Mater. Sci.*, **23**(5), P. 361–367 (2000).
[13] J. Mathew, S. Kurien, S. Sebastian, K.C. George, Dielectric studies of nanocrystalline copper orthophosphate. *Ind. J. Phys.*, **78**(9), P. 947–950 (2004).
[14] V. Murthy, K. Sobhanadri, Dielectric properties of some nickel-zinc ferrites at radio frequency. *Phys Status Solidi (a)*, **36**, P. K133 (1976).
[15] M.A.K.L. Dissanayake, O.A. Ileperuma, P.A.G.D. Darmasena, AC conductivity of $MnWO_4$. *J. Phys. Chem. Solids*, **50**, P. 359–361 (1989).
[16] R. Shukla, Electrical properties of $AgInTe_2$. *Ind. J. Pure Appl. Phys.*, **31**, P. 894–898 (1993).